

## Dynamical Effects of an Extended Cloud of Dark Matter on Dwarf Spheroidals

Ramanath Cowsik & Pranab Ghosh *Tata Institute of Fundamental Research, Homi Bhabha Road, Colaba, Bombay 400005*

Received 1985 April 4; accepted 1985 October 4

**Abstract.** If the dwarf spheroidals are embedded in an extended cloud of dark matter then their density profiles can be reproduced by assuming a Maxwellian distribution of velocities for the constituent stars. The observed luminosity profiles of dwarf spheroidals imply densities for the dark matter in the range  $10^{-26}$  to  $10^{-25}$  g cm $^{-3}$ , and mass-to-luminosity ratios which are typically an order of magnitude greater than those of globular clusters. Neutrinos of mass  $\sim 10$  eV and  $\langle v \rangle \sim 1000$  km s $^{-1}$  can provide this requisite density for the background.

*Key words:* galaxies, dark matter—galaxies, dwarf spheroidal—neutrino, mass

### 1. Introduction

The observation of high velocity dispersion of carbon stars in one dwarf spheroidal galaxy (Aaronson 1983) and considerations of the  $M/L$  ratios of dwarf spheroidals of the Local Group, based on tidal cut-off arguments (Faber & Lin 1983; Lin & Faber 1983) have indicated the presence of dark matter in these systems. In an earlier paper (Cowsik 1986) we have argued that the theoretical expectation of a high mass  $\gtrsim 400$  eV/ $c^2$  for the particles constituting this dark matter is an artifact of the assumption that the density distribution of the dark matter follows that of the visible matter and that if our Galaxy and the dwarf spheroidals are embedded in a neutrino condensation  $\sim 0.1$  Mpc in size, then  $m_\nu$ ,  $\sim 10$  eV can accommodate these observations. In this paper we investigate further this idea that the dwarf spheroidals are embedded in an extended cloud of dark matter and show that this model also predicts correctly the observed radial luminosity profiles (Hodge 1966 and references therein; Hodge & Michie 1969). The quality of the fit is so good as to lend strong support to the idea that neutrinos with a rest mass  $\sim 10$  eV/ $c^2$  generated copiously in the big bang triggered the initial condensations that led to the formation of the clusters of galaxies. In our picture, the visible matter in the form of spiral and elliptical galaxies, and dwarf spheroidals are embedded in these neutrino condensations, and through their gravitational dynamics delineate the distribution of the dark matter.

### 2. Calculation of self-consistent luminosity profiles

We assume that the velocity distribution of stars in a dwarf spheroidal is Maxwellian with typical velocity dispersion  $\sim 1$ – $10$  km s $^{-1}$ . Making use of a theorem due to Jeans

(Lynden-Bell 1962), the distribution function of the stars can be expressed as any function of their total energy  $E = \frac{1}{2} m_* v^2 + m_* \psi$ . Here  $\psi = \psi_v + \psi_*$  is the total gravitational potential due to the background neutrino gas and the stars. Thus

$$f(v) \sim \exp \left[ -\frac{m_*}{kT_*} \left( \frac{1}{2} v^2 + \psi_* + \psi_v \right) \right] \quad (1)$$

so that

$$\rho_* = \int f d^3v = \rho_0 \exp \left[ -\frac{m_*}{kT_*} (\psi_* + \psi_v) \right]. \quad (2)$$

The potentials satisfy the Poisson equation

$$\nabla^2 \psi = 4\pi G (\rho_* + \rho_v),$$

or

$$\nabla^2 \psi_* = 4\pi G \rho_* \quad \text{and} \quad \nabla^2 \psi_v = 4\pi G \rho_v, \quad (3)$$

with obvious notation. Now note that the typical length-scales for the spatial variations of the stars and neutrinos are given by

$$l_* \sim \left( \frac{kT_*}{4\pi G \rho_0 m_*} \right)^{1/2} \quad \text{and} \quad l_v \sim \left( \frac{kT_v}{4\pi G \rho_0 m_v} \right)^{1/2} \quad (4)$$

where  $\rho_0$  is the net central density. In the context of dwarf spheroidals embedded in an extended cloud of neutrinos we have  $\langle v_*^2 \rangle^{1/2} \simeq (3kT_*/m_*)^{1/2} \sim 1-10 \text{ km s}^{-1}$  and  $\langle v_v^2 \rangle^{1/2} \simeq (3kT_v/m_v)^{1/2} \sim 1000 \text{ km s}^{-1}$  so that  $l_v \gg l_*$ . This means that we can neglect the variation in the density of neutrinos over the extent of the dwarf spheroidals and set  $\rho_v \simeq \text{constant}$  in Equation (3).

Now we substitute Equation (1) in Equation (3), and make the resulting equation dimensionless by expressing the radial distance  $r$  from the centre of the dwarf spheroidal in units of the structural radius  $l_c = (kT_*/4\pi G \rho_c m_*)^{1/2}$ , i.e.,  $x = r/l_c$ , and the potentials in units of  $kT_*$ , i.e.,  $\phi_v = m_* \psi_v/kT_*$  and  $\phi_* = m_* \psi_*/kT_*$ . With these manipulations and the boundary condition on  $\phi_v$  that  $\phi_v(0) = 0$ , the equation for  $\phi_*$  becomes

$$x^{-2} (d/dx) (x^2 d\phi_*/dx) = \exp \left[ -\phi_* - \frac{1}{6} \frac{\rho_v}{\rho_c} x^2 \right]. \quad (5)$$

Here  $\rho_c$  is the central density of the stars. We obtain the solution of Equation (5), subject to the boundary condition  $\phi_*(0) = 0 = \phi'_*(0)$ , in a straightforward manner, following the method described by Emden (1907) and Chandrasekhar (1939).

Once  $\phi_*(r)$  is known, the Poisson equation yields  $\rho_*(r)$  and this can be projected to get the luminosity profile. We have with obvious notation,

$$\sigma(\mathbf{w}) = 2 \left\langle \frac{L_*}{m_*} \right\rangle \int_0^\infty \rho_* [(\mathbf{w}^2 + z^2)^{1/2}] dz. \quad (6)$$

### 3. Results

In Figs 1(a)-(f) we show the observed luminosity profiles of the six well-studied dwarf spheroidals of the Local Group (Hodge 1961a,b, 1962, 1963, 1964a, b, 1966; Hodge &

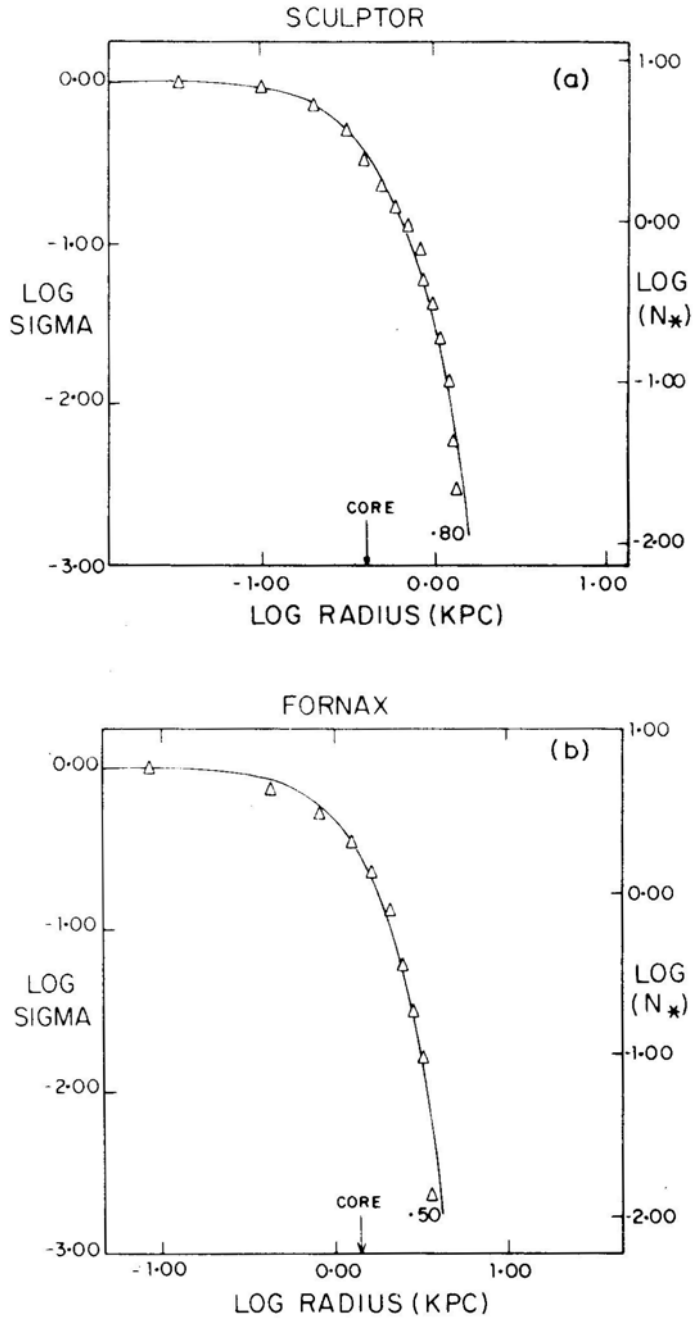


**Figure 1.** Surface density and star count profiles of: (a) Sculptor, (b) Fornax, (c) Leo I, (d) Leo II, (e) Draco, and (f) Ursa Minor, with the best fit model profiles, each model profile labelled by its value of  $\log(\rho_s/\rho_v)$ . Surface density (sigma) in units of its central value, and star count data are from Hodge (1961a, b, 1962, 1963, 1964a, b). Core radius is marked by arrow.

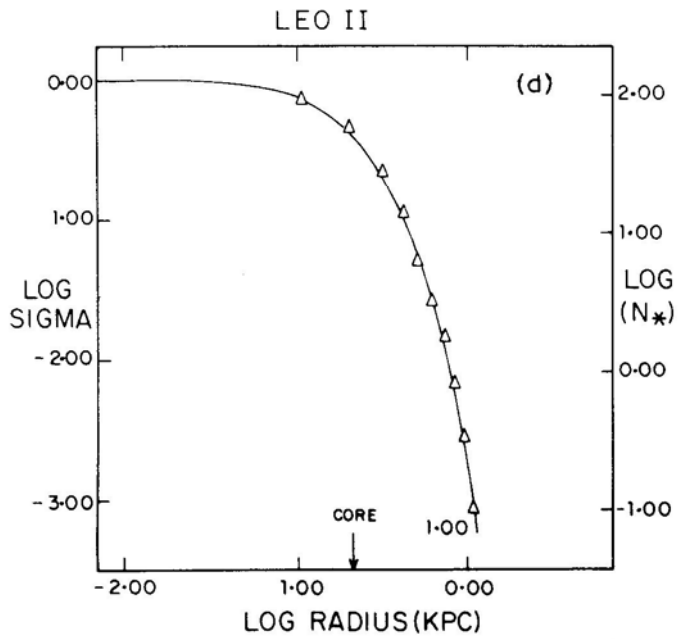
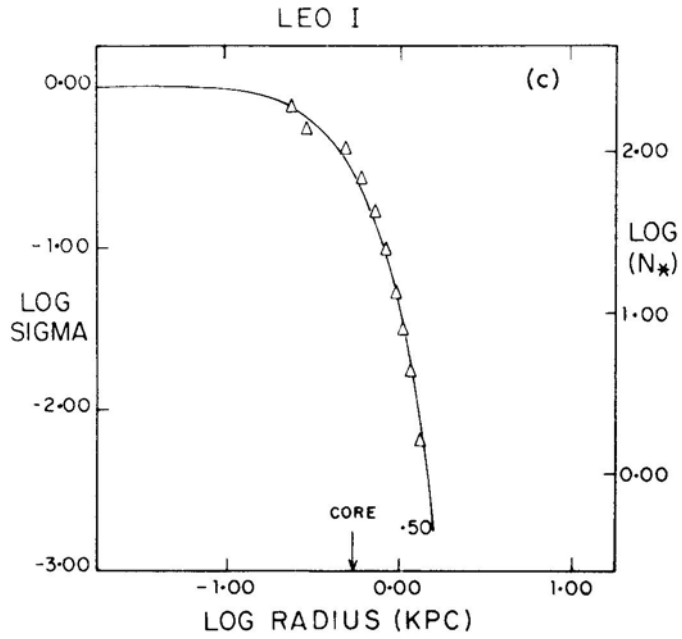


Figure 1. Continued.

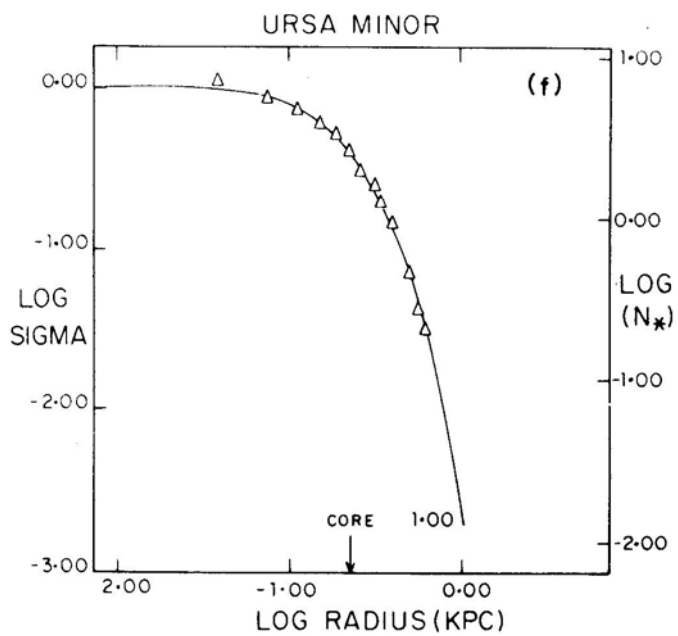
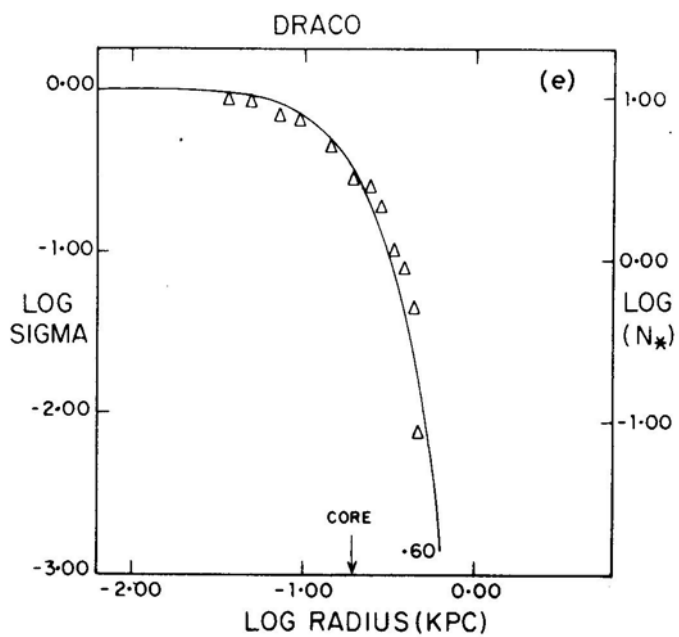


Figure 1. Continued.

Michie 1969) fitted by theoretical profiles. The fitting parameters are the core radius  $r_c = \langle v_*^2 \rangle^{1/2} / (4\pi G \rho_c / 3)^{1/2} = 3 l_c$  and the density ratio  $(\rho_c / \rho_v)$ . To obtain the 3-D velocity dispersion  $\langle v_*^2 \rangle^{1/2}$  and the neutrino density  $\rho_v$ , one needs an estimate of the central density  $\rho_c$ , which can be obtained by two methods: either (a) one can integrate our model to obtain the total visible mass and normalize to Hodge's (1966) value for this mass, or (b)<sup>†</sup> one can adopt the Lin-Faber (1983) value for the central surface brightness and assume a visible  $M/L = 2$ . In Table 1 we display the parameters obtained by the two methods: the second one gives somewhat higher  $\rho_c$ , and therefore larger  $\rho_v$  and  $\langle v_*^2 \rangle^{1/2}$ . (Note that the values of  $\rho_c$  in Table 1a are higher than those given by Hodge (1966) himself because there was a numerical error in his calculations. The corrected Hodge values are consistent with ours.) However, the important point is that both methods give a background density  $\rho_v (\sim 10^{-25} - 10^{-26} \text{ g cm}^{-3})$  which lies in the range of densities expected for the dark matter in the clusters of galaxies (Cowsik & Vasanthi 1986). In attributing this density of the background to neutrinos, we write

$$\rho_v \simeq \frac{8\pi g m_v \eta}{3} \left( \frac{m_v v_v}{h} \right)^3. \quad (7)$$

Here,  $v_v$  is the maximum velocity of the neutrinos and  $\eta$  is the fraction of the phase-space filled by them. For example, with  $g = 1$ ,  $\eta = 0.5$ ,  $m_v \simeq 10 \text{ eV}/c^2$  and  $v_v \simeq 1000 \text{ km s}^{-1}$ , Equation (7) yields  $\rho_v \simeq 10^{-24} \text{ g cm}^{-3}$ .

Now consider the velocity dispersion. (Note that line-of-sight dispersion =  $\langle v_*^2 \rangle^{1/2} / \sqrt{3}$ .) The values for Draco are somewhat lower than those reported by Aaronson (1983), while those for Fornax are in good agreement with those reported by Cohen (1983). The former discrepancy is unlikely to be significant because of the following uncertainties. On the one hand, Aaronson's measurements have insufficient statistics (3 stars measured, 2 only once), the measured stars may be in binaries, and Draco may be in the process of being disrupted (Hodge & Michie 1969). On the other, both methods of calculating  $\rho_c$  make use of the assumption that  $M$  (visible)/  $L$  for dwarf spheroidals and globular clusters is the same ( $\simeq 2$ ), which could be incorrect by an unknown amount.

The visible and dark components of the mass for a typical dwarf spheroidal galaxy in our model are shown in Fig. 2. The visible mass, which varies on a length-scale  $l_c$ , saturates by the limiting radius, whereas the dark mass, which varies on a much larger length scale (and is therefore nearly uniformly distributed on a scale  $l_c$ ) still increases like  $r^3$ . Inside the core of a dwarf spheroidal, the visible density dominates, while at the limiting radius, the total dark mass dominates the total visible mass. Indeed, the ratio of the *total* mass to the luminosity,  $M_{\text{tot}}/L$ , is typically an order of magnitude higher than the visible ( $M/L$ ) ratio (see Table 1). We emphasize two features of our model. First, the neutrino background does increase the central condensation and the velocity dispersion in DS galaxies, but this is done only indirectly by deepening the gravitational potential well in which the visible matter resides; the density and the velocity dispersion in the core of a dwarf spheroidal are still dominated by the visible matter contributions. Second, the velocity distribution in our model is not truncated, so that there is no upper limit to the allowed random velocity.

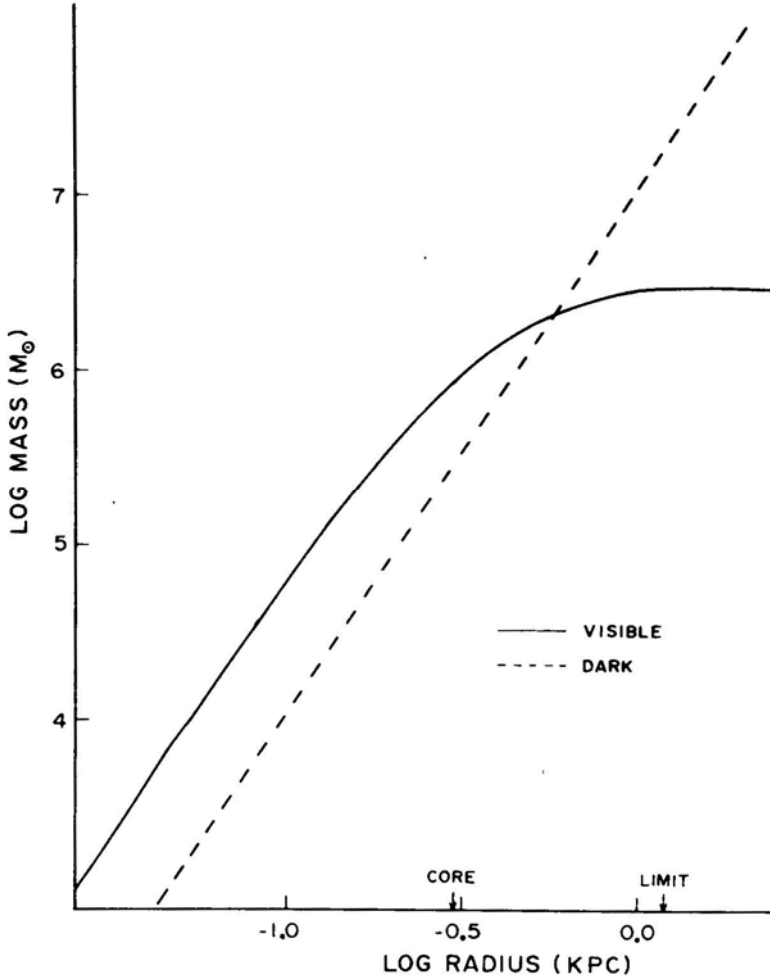
<sup>†</sup> We thank Dr S. Tremaine for pointing out the second method to us. Method (a) is in better accord with the recent observations.

Table 1. Parameters for Dwarf Spheroidal.

	Sculptor	Fornax	Leo I	Leo II	Draco	Ursa Minor
<b>(a) Method A: Using mass estimates.</b>						
Core radius, $R_c$ (kpc)	0.39	1.4	0.53	0.21	0.19	0.22
Limiting radius*, $R_L$ (kpc)	1.2	3.1	0.91	0.65	0.51	1.2
Visible mass*, $M_{vis}$ ( $M_\odot$ )	$3 \times 10^6$	$2 \times 10^7$	$4 \times 10^6$	$1 \times 10^6$	$1.2 \times 10^5$	$1 \times 10^5$
$\rho$ (visible) at centre ( $M_\odot/\text{pc}^3$ )	$7.1 \times 10^{-3}$	$1.7 \times 10^{-3}$	$6.0 \times 10^{-3}$	$1.3 \times 10^{-2}$	$3.5 \times 10^{-3}$	$1.1 \times 10^{-3}$
$\rho$ (dark) ( $\text{g cm}^{-3}$ )	$7.6 \times 10^{-26}$	$3.6 \times 10^{-26}$	$1.3 \times 10^{-25}$	$8.6 \times 10^{-26}$	$5.9 \times 10^{-26}$	$7.5 \times 10^{-27}$
$M_{\text{dark}}/M_{\text{vis}}$	6.2	12.4	8.5	1.8	12.5	10.1
Total mass, $M_{\text{tot}}$ ( $M_\odot$ )	$2.2 \times 10^7$	$2.7 \times 10^8$	$3.8 \times 10^7$	$2.8 \times 10^6$	$1.6 \times 10^6$	$1.1 \times 10^6$
$M_{\text{tot}}/L$ ratio ( $M_\odot/L_\odot$ )	14	27	19	6	27	22
3-D velocity dispersion, $\langle v_*^2 \rangle^{1/2}$ ( $\text{km s}^{-1}$ )	4.5	7.7	5.6	3.2	1.5	0.97
<b>(b) Method B: Using central surface brightness estimates.</b>						
Core radius, $R_c$ (kpc)	0.39	1.4	0.53	0.21	0.19	0.22
Limiting radius, $R_L$ (kpc)	1.2	3.1	0.91	0.65	0.51	1.2
Central surface brightness†	23.9	23.3	21.5	23.9	24.6	25.0
$m_v$ (mag arcsec $^{-2}$ )	$2.4 \times 10^{-2}$	$1.2 \times 10^{-2}$	$1.6 \times 10^{-1}$	$4.4 \times 10^{-2}$	$2.6 \times 10^{-2}$	$1.6 \times 10^{-2}$
$\rho$ (visible) at centre ( $M_\odot/\text{pc}^3$ )	$2.6 \times 10^{-25}$	$2.5 \times 10^{-25}$	$3.5 \times 10^{-24}$	$3.0 \times 10^{-25}$	$4.5 \times 10^{-25}$	$1.1 \times 10^{-25}$
$\rho$ (dark) ( $\text{g cm}^{-3}$ )	6.2	12.4	8.5	1.8	12.5	10.1
$M_{\text{dark}}/M_{\text{vis}}$	8.2	20	29	6.0	4.1	3.7
3-D velocity dispersion, $\langle v_*^2 \rangle^{1/2}$ ( $\text{km s}^{-1}$ )	14	27	19	6	27	22
$M_{\text{tot}}/L$ ratio ( $M_\odot/L_\odot$ ), assuming $M_{\text{vis}}/L = 2$						

\* Data taken from Hodge (1966).

† Data taken from Lin &amp; Faber (1983). Model (a) fits the recent observations on velocity dispersions better.



**Figure 2.** Visible and dark mass inside radius  $r$  for Sculptor. Visible mass dominates inside core. At limiting radius, dark mass (which goes as  $r^3$ ) dominates over visible mass (which saturates).

We conclude from this study that neutrinos with a mass of  $\sim 10 \text{ eV}/c^2$  can provide the requisite binding for the stars in the dwarf spheroidals provided the neutrino distribution extends to the typical dimensions of a cluster of galaxies. Exotic particles such as photinos, gravitinos and right-handed neutrinos with masses as high as  $500 \text{ eV}/c^2$  (Pagels & Primack 1981; Cabibbo, Farrar & Maiani 1981; Olive & Turner 1982) tend to condense on much smaller length-scales. Therefore these cannot explain in a simple way the profiles of luminosity of the spheroidals. The hypothesis that neutrinos have a mass of  $\sim 10 \text{ eV}/c^2$  naturally yields a density for the universe near closure (Gershtein & Zel'dovich 1966; Marx & Szalay 1972; Cowsik & McClelland 1972), a length- and mass-scale for condensations comparable to those of the clusters of galaxies (Cowsik & McClelland 1973; Bludman 1974; Schramm & Steigmann 1981), and also explains the dynamics of objects embedded in such condensations. Strictly speaking, any candidate for dark matter can be made to fit the observations if we adjust its density correctly and



allow it a velocity dispersion of  $1000 \text{ km s}^{-1}$ . But it is only for the neutrinos that this condition is naturally satisfied in a big-bang universe.

### References

- Aaronson, M. 1983, *Astrophys. J.*, **266**, L11.  
Bludman, S. A. 1974, in *Proc. Neutrino 74*, **1**, 284.  
Cabibbo, N., Farrar, G. R., Maiani, L. 1981, *Phys. Lett.*, **105B**, 155.  
Chandrasekhar, S. 1939, in *An Introduction to the Study of Stellar Structure*, Univ. Chicago Press, p 156.  
Cohen, J. G. 1983, *Astrophys. J.*, **270**, L41.  
Cowsik, R. 1986, *J. Astrophys. Astr.*, **7**, 1.  
Cowsik, R., Vasanthi, M. 1986, *J. Astrophys. Astr.*, **7**, 29.  
Cowsik, R., McClelland, J. 1972, *Phys. Rev. Lett.*, **29**, 669.  
Cowsik, R., McClelland, J. 1973, *Astrophys. J.*, **180**, 7.  
Emden, R. 1907, *Gaskugeln*, Leipzig, Teubner.  
Faber, S. M., Lin, D. N. C. 1983, *Astrophys. J.*, **266**, L17.  
Gershtein, S. S., Zel'dovich, Ya, B. 1966, *JETP Letters*, **4**, 174.  
Hodge, P. W. 1961a, *Astr. J.*, **66**, 249.  
Hodge, P. W. 1961b, *Astr. J.*, **66**, 384.  
Hodge, P. W. 1962, *Astr. J.*, **67**, 125.  
Hodge, P. W. 1963, *Astr. J.*, **68**, 470.  
Hodge, P. W. 1964a, *Astr. J.*, **69**, 438.  
Hodge, P. W. 1964b, *Astr. J.*, **69**, 853.  
Hodge, P. W. 1966, *Astrophys. J.*, **144**, 869.  
Hodge, P. W., Michie, R. W. 1969, *Astr. J.*, **74**, 587.  
Lin, D. N. C., Faber, S. M. 1983, *Astrophys. J.*, **266**, L21.  
Lynden-Bell, D. 1962, *Mon. Not. R. astr. Soc.*, **124**, 95.  
Marx, G., Szalay, A. S. 1972, *Proc. Neutrino 72*, Technoinform, Hungary, **1**, 123.  
Olive, K. A., Turner, M. S. 1982, *Phys. Rev.*, **D25**, 213.  
Pagels, H., Primack, J. R. 1982, *Phys. Rev. Lett.*, **48**, 223.  
Schramm, D. N., Steigman, G. 1981, *Astrophys. J.*, **243**, 1.